Inorganic Chemistry

ARTICLE

pubs.acs.org/IC

Low-Temperature Vacuum Reduction of $BiMnO_3$

Alexei A. Belik,*[,†] Yoshitaka Matsushita,[‡] Masahiko Tanaka,[‡] and Eiji Takayama-Muromachi[†]

[†]International Center for Materials Nanoarchitectonics (MANA), National Institute for Materials Science (NIMS), 1-1 Namiki, Tsukuba, Ibaraki 305-0044, Japan

[‡]SPring-8 Office, National Institute for Materials Science (NIMS), Kohto 1-1-1, Sayo-cho, Hyogo 679-5148, Japan

Supporting Information

ABSTRACT: Low-temperature vacuum reduction was used for the preparation of the oxygen-deficient $BiMnO_{2.81}$ sample in a bulk form from stoichiometric $BiMnO_3$. The transformation occurs in vacuum better than 10^{-3} Pa at a narrow temperature range of 570−600 K. The structure of the new phase was analyzed using synchrotron X-ray powder diffraction data. $BiMnO_{2.81}$ crystallizes in a perovskite-type cubic structure (space group $I-43d$) with a = 15.88552(5) Å corresponding to a $4a_p$ superstructure, where a_p is the parameter of the cubic perovskite subcell. Oxygen vacancies are ordered, and one oxygen site in $BiMnO_{2.81}$ is completely vacant, resulting in MnO_5 pyramids. $BiMnO_{2.81}$ is rather unstable in air and slowly restores its oxygen content even at room temperature.

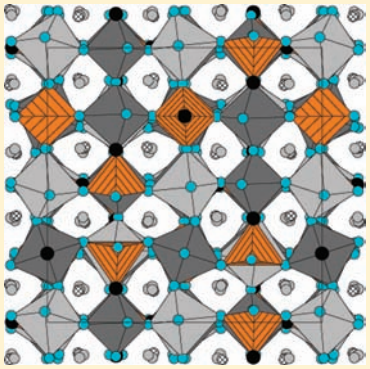

1. INTRODUCTION

Transition metal oxides are very important for both fundamental and applied sciences. Their structural and physical properties are usually modified/improved by cation and anion doping. The oxygen content is known to have crucial and dramatic roles on the properties of materials, for example, on magnetic and electronic properties of perovskites (e.g., $LaMnO_{3+\delta}$,[1−4] $BiMnO_{3+\delta}$,[5−7] $(BiMn_3)Mn_4O_{12}$,[8] and $Sr_{1-x}Y_xCoO_{3+\delta}$)[9] and high-temperature copper superconductors (e.g., $YBa_2Cu_3O_{7+\delta}$).[10] In $LaMnO_{3+\delta}$,[1−4] the change of δ results in changes from an antiferromagnetic insulator to a ferromagnetic insulator to a ferromagnetic metal; at the same time, crystal symmetries are also changed from *Pnma*(I) to *Pnma*(II) to *R*−3*c*. In $BiMnO_{3+\delta}$,[6,7] the change of δ results in changes from ferromagnetic insulators to a spin-glass insulator; crystal structures change from $C2/c$(I) to $C2/c$(II) to $P2_1/c$ to *Pnma*(II). Note that even though the formula is written as $LaMnO_{3+\delta}$ or $BiMnO_{3+\delta}$ for simplicity, cation vacancies $La_{1-x}Mn_{1-x}O_3$ or $Bi_{1-x}Mn_{1-x}O_3$ are actually formed in perovskite structures.

Direct high-temperature syntheses of $LaMnO_{3+\delta}$ (in different atmospheres)[1−4] or high-pressure high-temperature syntheses of $BiMnO_{3+\delta}$ result in oxygen hyperstoichiometric samples ($\delta \geq 0$).[6] It was believed for some time that $LaMnO_3$ with oxygen deficiency could not be prepared.[11] However, methods have later been found to synthesize the oxygen-deficient $LaMnO_{3-\delta}$ samples (e.g., $LaMnO_{2.75}$) by zircothermal reduction of $LaMnO_3$ or very careful reduction of $LaMnO_3$ with H_2 at low temperatures.[11] The oxygen content can be lowered by other methods. For example, the topotactic reduction at low temperatures became very popular and allows access to unusual structures, e.g., $SrFeO_2$ from $SrFeO_3$,[12] $Yb_2Ti_2O_{6.43}$ from $Yb_2Ti_2O_7$,[13] and $YBaCo_2O_{4.5}$ from $YBaCo_2O_5$.[14] Annealing at different atmospheres or in vacuum is another method (e.g., used for $Bi_3Mn_3O_{11-\delta}$).[15] Some reduced phases (which are usually thermodynamically stable) can be prepared either by lowering the oxygen content of oxidized samples or by direct syntheses in oxygen-free environments (in an Ar flow, in evacuated tubes, and so on) from appropriate precursors, e.g. $Sr_2Fe_2O_5$.[16] Thermodynamically unstable reduced phases can be prepared by lowering the oxygen content of oxidized samples.[14]

In the case of oxygen-deficient $BiMnO_{3-\delta}$, direct synthesis methods were unsuccessful.[6] Generally, the use of strongly reducing agents (H_2 or those used in the topotactic reduction methods) is not favorable for Bi- and Pb-based oxides because these ions are very easily reduced to the metal state. Therefore, soft reduction methods should be applied for preparation of $BiMnO_{3-\delta}$. In this work, we found such a method, which includes a treatment of stoichiometric $BiMnO_3$ in vacuum better than 10^{-3} Pa at low temperatures of 570−600 K. This method gives an oxygen-deficient sample with the composition of $BiMnO_{2.81}$. $BiMnO_{2.81}$ is rather unstable in air and slowly restores its oxygen content even at room temperature. The preparation method may be promising for reduction of the oxygen content in other Bi- and Pb-based oxides.

2. EXPERIMENTAL SECTION

$BiMnO_3$ was prepared from stoichiometric mixtures of Bi_2O_3 (99.9999%, Rare Metallic Co. Ltd.) and Mn_2O_3 (99.99%). Synthesis of $BiMnO_3$

Received: April 7, 2011
Published: July 12, 2011

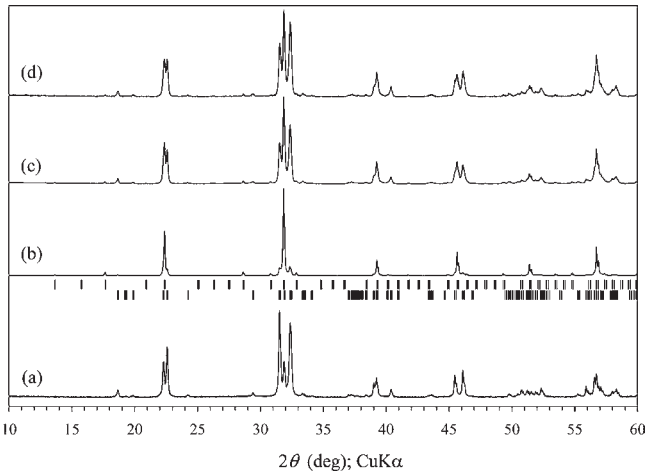

Figure 1. Room-temperature X-ray powder diffraction patterns (measured with Cu Kα radiation) of (a) the stoichiometric $BiMnO_3$, (b) R-$BiMnO_{3-\delta}$ (after treatment of $BiMnO_3$ in the dynamic vacuum of 10^{-4}−10^{-3} Pa at 570−600 K for 5 h), (c) the 13-month-old R-$BiMnO_{3-\delta}$, and (d) the 24-month-old R-$BiMnO_{3-\delta}$. Tick marks in b show positions of possible Bragg reflections for $BiMnO_{2.81}$ (space group $I-43d$) (first row) and $BiMnO_3$ (space group $C2/c$) (second row).

was performed in a belt-type high-pressure apparatus at 6 GPa and 1600 K for 40 min in sealed Pt capsules. After heat treatment, the samples were quenched to room temperature and the pressure was slowly released.[17] Stoichiometric $BiMnO_3$ was then treated in the dynamic vacuum of 10^{-4}−10^{-3} Pa at 570−600 K for 5 h.

X-ray powder diffraction (XRD) data were collected at room temperature on a RIGAKU Ultima III diffractometer using Cu Kα radiation (2θ range of 4−100°, step width of 0.02°, and counting time of 2−10 s/step). Synchrotron XRD data were measured at room temperature on a large a Debye−Scherrer camera at the BL15XU beamline of SPring-8.[18] The data were collected between 5° and 60° at a 0.003° interval in 2θ. The incident beam was monochromatized at $\lambda = 0.40039$ Å. The sample was packed into a Lindenmann glass capillary (i.d. 0.1 mm), which was rotated during the measurement. Rietveld analysis was performed with RIETAN-2000.[19] The weight fraction of different phases was estimated based on the refined scale factors in Rietveld analysis.

Magnetic susceptibilities, $\chi = \mathbf{M}/\mathbf{H}$, were measured on a SQUID magnetometer (Quantum Design, MPMS-5T) between 2 and 300 K in different applied fields under both zero-field-cooled (ZFC) and field-cooled (FC) conditions. Thermogravimetric analysis (TGA) was performed in air using a Perkin-Elmer Pyris 1 TGA system in an Al_2O_3 holder (the samples were heated to 640 K at a heating rate of 5 K/min and soaked there for 30 min).

3. RESULTS AND DISCUSSION

Figure 1a shows the XRD pattern of stoichiometric $BiMnO_3$. $BiMnO_3$ crystallizes in the $C2/c$ space group with lattice parameters of $a = 9.5415(2)$ Å, $b = 5.61263(8)$ Å, $c = 9.8632(2)$ Å, and $\beta = 110.6584(12)°$.[17] Figure 1b depicts the XRD pattern of a sample just after treatment in vacuum of 10^{-4}−10^{-3} Pa at 570−600 K for 5 h. This sample will be called R-$BiMnO_{3-\delta}$, and it consisted of $BiMnO_3$ with the $C2/c$ space group (about 20 wt %) and a new phase $BiMnO_{2.81}$ (the composition determination will be given below) having a cubic symmetry (about 80 wt %). Figure 1c and 1d shows the XRD patterns of R-$BiMnO_{3-\delta}$ after keeping it in dry air at room temperature for 13 and 24 months, respectively. The 13-month-old sample consisted of $BiMnO_3$ (about 67 wt %) and $BiMnO_{2.81}$ (about 33 wt %), and the 24-month-old sample consisted of $BiMnO_3$ (about 78 wt %) and $BiMnO_{2.81}$ (about 22 wt %).

All our attempts (that lasted for more than 2 years and resulted in Figure 1c and 1d) to increase the weight fraction of $BiMnO_{2.81}$ failed. However, using high-resolution synchrotron XRD data we could obtain reliable structural information for $BiMnO_{2.81}$ even for the two-phase sample. When $BiMnO_3$ was treated in vacuum of 10^{-4}−10^{-3} Pa at a slightly higher temperature of 670 K the sample partially decomposed to give monoclinic Bi_2O_3 as an impurity (with disappearance of the cubic phase). The vacuum treatment at 800 K resulted in complete sample decomposition (identified phases were Mn_3O_4, $Bi_2Mn_4O_{9+\delta}$, $Bi_{12}MnO_{20+\delta}$, and monoclinic Bi_2O_3). When the temperature was lower than 530 K (at 10^{-4}−10^{-3} Pa) or when vacuum was worse than 10^{-3} Pa (at any temperatures) the cubic phase did not appear. We could not find the appearance of the cubic phase at any conditions in a slightly Bi-deficient sample of $Bi_{0.97}Mn^{3+}O_{2.955}$.

The above results demonstrate that (1) stabilization of $BiMnO_{2.81}$ can be achieved in a very narrow temperature range and only in the Bi:Mn = 1:1 stoichiometric sample and (2) the oxygen-deficient $BiMnO_{2.81}$ sample is rather unstable in air. $BiMnO_{2.81}$ slowly restores its oxygen content to form $BiMnO_3$. Instability of $BiMnO_{2.81}$ in air is a possible reason why $BiMnO_{2.81}$ could not be prepared/observed in a single-phase form. It is possible that the surface area of $BiMnO_{2.81}$ is oxidized very fast to give $BiMnO_3$, and then the oxidation process proceeds very slowly at room temperature. Thermodynamic instability of $BiMnO_{2.81}$ explains why the oxygen-deficient samples cannot be prepared by direct high-pressure high-temperature synthesis;[6] during synthesis, samples restore their oxygen content by different ways to give $BiMnO_3$.

Magnetic measurements of R-$BiMnO_{3-\delta}$ showed two anomalies: at 100 K due to a ferromagnetic transition in $BiMnO_3$ and an antiferromagnetic-like anomaly at 26 K (see the Supporting Information). The anomaly near 26 K can be assigned to $BiMnO_{2.81}$.

All reflections on the XRD pattern of R-$BiMnO_{3-\delta}$ (except those of $BiMnO_3$) could be indexed in the I-centered cubic system with $a = 15.8855$ Å. The structural model for $BiMnO_{2.81}$ was obtained from a simple cubic perovskite structure with $a_p = 3.9$ Å and space group $Pm-3m$ (No. 221). All possible I-centered cubic space groups with $a = 4a_p$ have been generated and tested. The best agreement between the observed and the calculated synchrotron XRD patterns and the fitting of all weak reflections have been achieved in space group $I-43d$ (No. 220). Therefore, the final refinement of $BiMnO_{2.81}$ was performed in space group $I-43d$. The final fractional coordinates and other structural parameters are given in Table 1 and selected bond lengths in Table 2. Observed, calculated, and difference synchrotron XRD patterns are shown in Figure 2. Figure 3 depicts the crystal structure of $BiMnO_{2.81}$. The structural parameters for the impurity $BiMnO_3$ phase were also refined, and they were found to be very reasonable and rather close to those reported in the literature.[17] One generated oxygen site (O6 at the 12a site (3/8,0,1/4)) in $BiMnO_{2.81}$ was found to be completely vacant. Other sites (except for O1) had reasonable displacement thermal parameters (B), indicating that these sites should be fully occupied. The O1 site should be discussed in more detail. Attempts to refine its occupation factor, g, together with the B(O1) parameter did not reduce B(O1) and left g(O1) very close to unity. The O1 site was then split from the ideal 24d site (x, 0, 1/4) with $g = 1$ to a general 48e site (x, y, z) with $g = 0.5$. The refined parameters were $x = 0.645(3)$, $y = 0.031(4)$, $z = 0.282(4)$, and

dx.doi.org/10.1021/ic2007233 |Inorg. Chem. 2011, 50, 7685–7689

Table 1. Structure Parameters of $BiMnO_{2.81}$ at 293 K in the Ordered Model[a]

site	g	x	y	z	B (Å^2)
Bi1	1	0.36278(11)	= x	= x	0.84(6)
Bi2	1	0.13248(12)	0.36782(12)	0.87991(15)	0.73(2)
Mn1	1	0.2473(9)	= x	= x	0.6(3)
Mn2	1	0.2483(10)	0	0.25	0.6(3)
Mn3	1	0.0043(8)	0	0.25	0.6(3)
O1	1	0.628(4)	0	0.25	9.8(2.4)
O2	1	0.875	0	0.25	0.4(4)
O3	1	0.1326(18)	0.7076(14)	0.5019(14)	0.4(4)
O4	1	0.1326(14)	−0.0082(13)	0.0380(13)	0.4(4)
O5	1	0.7273(15)	0.3814(23)	0.2573(14)	0.4(4)

[a] Space group $I-43d$ (No 220); $Z = 64$; $a = 15.88552(5)$ Å and $V = 4008.70(2)$ Å^3, $R_{wp} = 4.98\%$, $R_p = 3.27\%$, $R_B = 3.06\%$, and $R_F = 1.79\%$. $R_B = 2.29\%$, and $R_F = 1.54\%$ for the monoclinic $BiMnO_3$ phase. g is the occupation factor, and B is the isotropic thermal parameter.

Table 2. Selected Bond Lengths, l (Å), Bond Valence Sums, BVS, and Distortion Parameters of MnO_6, Δ, in $BiMnO_{2.81}$ in the Ordered Model[a]

Bi1−O4 (×3)	2.281(19)	Bi2−O3	2.227(24)
Bi1−O1 (×3)	2.826(20)	Bi2−O5	2.313(20)
BVS($Bi1^{3+}$)	2.22	Bi2−O4	2.325(23)
BVS($La1^{3+}$)	2.75	Bi2−O3	2.373(21)
		Bi2−O5	2.669(25)
		Bi2−O2	2.818(2)
		Bi2−O1	2.945(20)
		Bi2−O5	3.169(25)
		BVS($Bi2^{3+}$)	2.77
Mn1−O5 (×3)	2.091(36)	Mn3−O1	1.875(73)
Mn1−O4 (×3)	2.245(28)	Mn3−O4 (×2)	1.970(23)
		Mn3−O2	2.054(13)
BVS($Mn1^{3+}$)	2.04	Mn3−O3 (×2)	2.214(29)
BVS($Mn1^{2+}$)	2.21	BVS($Mn3^{3+}$)	2.91
Δ($Mn1O_6$)	12.7×10^{-4}	Δ($Mn3O_6$)	38.5×10^{-4}
Mn2−O5 (×2)	1.927(35)		
Mn2−O3 (×2)	1.993(29)		
Mn2−O1	2.001(74)		
BVS($Mn2^{3+}$)	2.86		

[a] BVS = $\Sigma_{i=1}^{N} v_i$, $v_i = \exp[(R_0 - l_i)/B]$, N is the coordination number, $B = 0.37$, $R_0(Bi^{3+}) = 2.094$, $R_0(La^{3+}) = 2.172$, $R_0(Mn^{3+}) = 1.76$, and $R_0(Mn^{2+}) = 1.79$.[21] $\Delta = (1/N) \Sigma_{i=1}^{N} [(l_i - l_{av})/l_{av}]^2$, where $l_{av} = (1/N) \Sigma_{i=1}^{N} l_i$ is the average Mn−O distance.

$B(O1) = 1.6(1.3)$ Å^2 (see Supporting Information). The $B(O1)$ parameter obtained is acceptable. Therefore, we assumed that there are no additional vacancies at the O1 site. The $BiMnO_{2.8125}$ composition was calculated assuming that only the O6 site is completely vacant. This composition leads to the following oxidation states, $Bi^{3+}Mn^{2+}_{0.375}Mn^{3+}_{0.625}O_{2.8125}$.

Neutron powder diffraction is the best method for determination of positions and occupation factors of oxygen atoms. However, neutron powder diffraction usually requires a large volume of a sample. We emphasize that high-resolution synchrotron X-ray powder diffraction is also rather sensitive. In the present case, the forced introduction of the O6 atom (with $g = 1$)

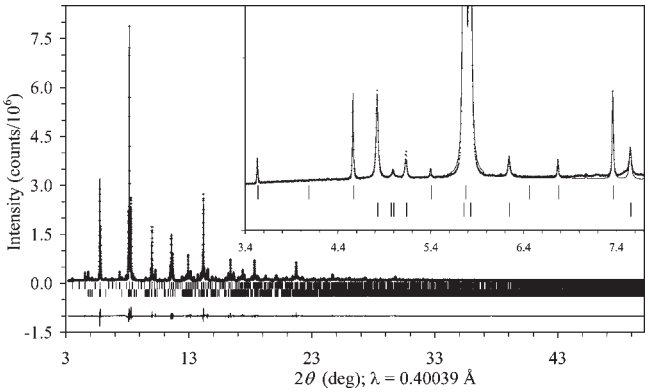

Figure 2. Observed (crosses), calculated (solid line), and difference synchrotron X-ray powder diffraction patterns of R-$BiMnO_{3-\delta}$. Tick marks show positions of possible Bragg reflections for $BiMnO_{2.81}$ (space group $I-43d$) (first row) and $BiMnO_3$ (space group $C2/c$) (second row). (Insert) Enlarged fragment.

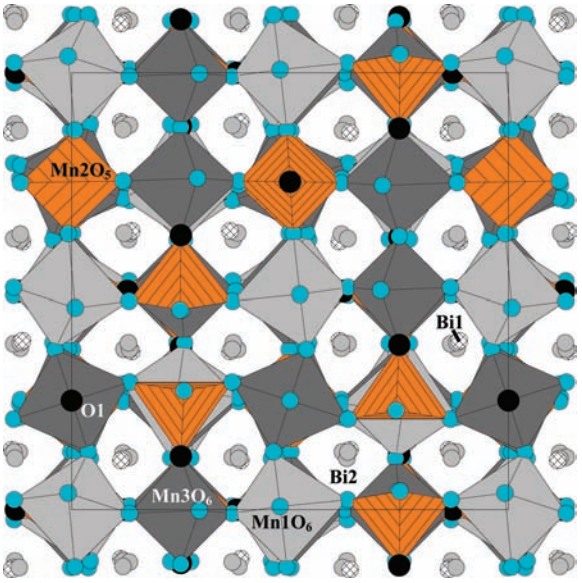

Figure 3. Crystal structure of $BiMnO_{2.81}$.

and refinements of all other parameters slightly increased R values to $R_{wp} = 5.05\%$, $R_p = 3.33\%$, $R_B = 3.26\%$, and $R_F = 1.89\%$ from $R_{wp} = 4.98\%$, $R_p = 3.27\%$, $R_B = 3.06\%$, and $R_F = 1.79\%$. Most importantly, the subsequent refinement of g(O6) gave a negative value, indicating that this site is vacant. The forced removal of an existing O atom (with $g = 0$) and refinements of all other parameters also increased R values (e.g., to $R_{wp} = 5.06\%$, $R_p = 3.33\%$, $R_B = 3.24\%$, and $R_F = 2.02\%$ for O2). However, a subsequent refinement of the occupation factor resulted in a value close to unity. Reasonable bond lengths and bond-valence sum values (see below) also justify the structural model obtained from synchrotron X-ray powder diffraction data.

In $BiMnO_{2.81}$, the Mn1 and Mn3 sites keep the octahedral coordination. For the Mn2 site, one corner of the octaderon is missing (the O6 site), leading to a square pyramidal coordination. The O3 and O5 sites form the basis of the pyramid, and the O1 site is an apex. The O1 site is opposite to the missing O6 site (that is, the O1−Mn2−O6 angle is close to 180°). This is a

dx.doi.org/10.1021/ic2007233 |Inorg. Chem. 2011, 50, 7685–7689

possible reason for the disordering of the O1 site because the missing O6 site should create distortions around the Mn2 site. A square pyramidal coordination was observed in $La_{0.33}Sr_{0.67}MnO_{2.42}$ but with the random distribution of vacancies in octahedral layres.[20]

The bond-valence sum (BVS)[21] parameters in $BiMnO_{2.81}$ were calculated to be +2.04 for Mn1, +2.86 for Mn2, +2.91 for Mn3, +2.22 for Bi1, and +2.77 for Bi2 (Table 2). There are four short Mn2−O (1.875−2.054 Å) and two long Mn3−O3 (2.214 Å) distances indicating the presence of a strong Jahn−Teller distortion of the $Mn3O_6$ octahedron. This fact coupled with the BVS(Mn3) parameter shows that the Mn3 site should be exclusively occupied by Mn^{3+} ions. The BVS(Mn1) parameter suggests that the Mn1 site is occupied by Mn^{2+} ions. The Mn2 site should have mixed Mn^{2+}/Mn^{3+} oxidation states. The significantly reduced BVS parameters for Bi^{3+} were found in $BiMn_7O_{12}$ (BVS(Bi) = +2.22)[22] and $BiMnO_{3.14}$ (BVS(Bi) = +2.35).[7] It seems that the effect of the lone electron pair of Bi^{3+} is vanished in $BiMn_7O_{12}$ and $BiMnO_{3.14}$, and Bi^{3+} ions behave similar to La^{3+} ions in these compounds (when $R_0(La^{3+}) = 2.172$ was used for the calculation of the BVS parameters instead of $R_0(Bi^{3+}) = 2.094$, the BVS(Bi) parameters became reasonable). A similar behavior is probably observed for the Bi1 site in $BiMnO_{2.81}$.

Oxygen-deficient $ABO_{3-\delta}$-type compounds often have the octahedral and tetrahedral coordinations of the *B*-type cations with ordered arrangements of BO_6 octahedra and BO_4 tetrahedra resulting in brownmillerite-related polyhedral arrangmetns.[9,16,20,23] The concentration of oxygen vacancies in $BiMnO_{2.81}$ and the synthesis temperature are probably not enough to cause a significant structural reconstruction from MnO_6 octahedra to MnO_4 tetrahedra. Therefore, $BiMnO_{2.81}$ keeps a perovskite-type motif instead of a brownmillerite-type motif. The presence of MnO_5 pyramids and underbonded Bi^{3+} ions in $BiMnO_{2.81}$ are possible reasons for its instability in air. Instability of $BiMnO_{2.81}$ is in agreement with a general tendency that phases formed by low-temperature reduction methods are highly metastable.[14] The preparative approach of $BiMnO_{2.81}$ may look rather complicated, similar to the topotactic reduction method. The latter includes a preparation of initial oxidized samples, then a low-temperature solid-state reaction with reducing agents, and finally removing unnecessary phases. However, vacuum soft reduction of $BiMnO_3$ or topotactic reduction methods seem to be the only way to some exotic and metastable materials. Reduced phases may have excellent practical properties.[24]

We note that an oxygen-deficient modification of $BiMnO_3$ (having an *I*-centered cubic symmetry with $a \approx 15.9$ Å) was observed inside electron microscopes.[25−31] This observation was first assigned to the intrinsic coexistence of two modifications of $BiMnO_3$.[25,26] Later it was believed that the electron beam knocked out the oxygen from the lattice.[27,28] Electron diffraction observations confirm the space group we selected. However, the reduced modification has never been stabilized outside of electron microscopes so far. Therefore, its chemical composition, crystal structure, and physical properties have not been known. Our results showed that the high vacuum inside electron microscopes (on the order of 10^{-6} Pa) is the main reason for the transformation, and the electron beam just plays the role of a heater. The transformation inside electron microscopes was easily observed. This fact shows that the vacuum on the order of 10^{-6} Pa (not reachable with our equipment) might be better for preparation of $BiMnO_{2.81}$. Compositional and structural changes in $BiMnO_3$ under vacuum show that results of electron diffraction studies on $BiMnO_3$ should be interpreted with care. When a rather weak electron beam was used for the measurements the crystal symmetry of $BiMnO_3$ was determined to be $C2/c$.[17] With a stronger beam, additional weak spots on electron diffraction patterns have been observed corresponding to a long-range-ordered structure with the *C*2 symmetry and a short-range-ordered structure with the *P*2 or $P2_1$ symmetry.[32] The presence of the additional spots could be either intrinsic or just caused by an initial transformation inside an electron microscope. With longer exposure time,[27] the monoclinic-to-cubic transformation occurs.[25−31]

$BiMnO_{2.81}$ crystallizes in space group $I-43d$ (No. 220) belonging to noncentrosymmetric-nonpolar crystal classes.[33] This crystal class supports piezoelectric and second-harmonic-generation properties (for example, piezoelectric $Bi_4Ge_3O_{12}$ crystallizes in space group $I-43d$)[34] but does not support ferroelectric properties. Therefore, the appearance of oxygen-deficient $BiMnO_{2.81}$ in inner layers of thin films during film growth under the reduced pressure may be one of the reasons for the observation of a large nonlinear optical response in some thin-film samples of $BiMnO_{3\pm\delta}$.[35] We note that the existence of ferroelectric properties of $BiMnO_3$ is still a matter of debate in the literature. First-principle calculations confirmed the centrosymmetric $C2/c$ space group for the ideal $BiMnO_3$.[36] Ferroelectric hysteresis loops have not been observed in many well-characterized thin film and bulk $BiMnO_3$ samples, in agreement with the centrosymmetric crystal structure. Unfortunately, these 'negative' results usually are not published. Thin-film samples that do show ferroelectric hysteresis loops usually demonstrate different magnetic properties (the reduced ferromagnetic Curie temperature and strongly reduced saturated magnetization) compared with properties of the bulk stoichiometric $BiMnO_3$.[37]

In conclusion, we found a method for preparation of oxygen-deficient $BiMnO_{2.81}$ in the bulk form and could investigate its structural properties. Structural analysis showed that oxygen vacancies are ordered, and one oxygen site in $BiMnO_{2.81}$ is completely vacant, resulting in MnO_5 pyramids. $BiMnO_{2.81}$ is rather unstable in air and slowly restores its oxygen content even at room temperature.

■ ASSOCIATED CONTENT

Supporting Information. Structural parameters of $BiMnO_{2.81}$ in the disordered model, and thermogravimetric and magnetic susceptibility curves of R-$BiMnO_{3-\delta}$. This material is available free of charge via the Internet at http://pubs.acs.org.

■ AUTHOR INFORMATION

Corresponding Author

*E-mail: Alexei.Belik@nims.go.jp.

■ ACKNOWLEDGMENT

This work was supported by World Premier International Research Center (WPI) Initiative on Materials Nanoarchitectonics (MEXT, Japan), by the NIMS Individual-Type Competitive Research Grant, by the Japan Society for the Promotion of Science (JSPS) through its "Funding Program for World-Leading Innovative R&D on Science and Technology (FIRST

Program)", and by the Grants-in-Aid for Scientific Research (22246083) from JSPS, Japan. The synchrotron radiation experiments were performed at the SPring-8 with the approval of the Japan Synchrotron Radiation Research Institute (Proposal nos. 2009A4800 and 2009B4505). We thank Dr. A. M. Abakumov for discussion.

REFERENCES

(1) Alonso, J. A.; Martinez-Lope, M. J.; Casais, M. T.; MacManus-Driscoll, J. L.; de Silva, P. S. I. P. N.; Cohen, L. F.; Fernandez-Diaz, M. T. *J. Mater. Chem.* **1997**, *7*, 2139.
(2) Huang, Q.; Santoro, A.; Lynn, J. W.; Erwin, R. W.; Borchers, J. A.; Peng, J. L.; Greene, R. L. *Phys. Rev. B* **1997**, *55*, 14987.
(3) Topfer, J.; Goodenough, J. B. *J. Solid State Chem.* **1997**, *130*, 117.
(4) Maurin, I.; Barboux, P.; Lassailly, Y.; Boilot, J. P.; Villain, F.; Dordor, P. *J. Solid State Chem.* **2001**, *160*, 123.
(5) Sundaresan, A.; Mangalam, R. V. K.; Iyo, A.; Tanaka, Y.; Rao, C. N. R. *J. Mater. Chem.* **2008**, *18*, 2191.
(6) Belik, A. A.; Kolodiazhnyi, T.; Kosuda, K.; Takayama-Muromachi, E. *J. Mater. Chem.* **2009**, *19*, 1593.
(7) Belik, A. A.; Kodama, K.; Igawa, N.; Shamoto, S.; Kosuda, K.; Takayama-Muromachi, E. *J. Am. Chem. Soc.* **2010**, *132*, 8137.
(8) Imamura, N.; Karppinen, M.; Yamauchi, H. *Chem. Mater.* **2009**, *21*, 2179.
(9) Ishiwata, S.; Kobayashi, W.; Terasaki, I.; Kato, K.; Takata, M. *Phys. Rev. B* **2007**, *75*, 220406(R).
(10) Strobel, P.; Capponi, J. J.; Chaillout, C.; Marezio, M.; Tholence, J. L. *Nature* **1987**, *327*, 306.
(11) Ruiz-Gonzalez, M. L.; Cortes-Gil, R.; Alonso, J. M.; Hernando, A.; Vallet-Regi, M.; Gonzalez-Calbet, J. M. *Chem. Mater.* **2006**, *18*, 5756 and references therein.
(12) Tsujimoto, Y.; Tassel, C.; Hayashi, N.; Watanabe, T.; Kageyama, H.; Yoshimura, K.; Takano, M.; Ceretti, M.; Ritter, C.; Paulus, W. *Nature* **2007**, *450*, 1062.
(13) Blundred, G. D.; Bridges, C. A.; Rosseinsky, M. J. *Angew. Chem., Int. Ed.* **2004**, *43*, 3562.
(14) Seddon, J.; Suard, E.; Hayward, M. A. *J. Am. Chem. Soc.* **2010**, *132*, 2802.
(15) Belik, A. A.; Takayama-Muromachi, E. *J. Am. Chem. Soc.* **2010**, *132*, 12426.
(16) D'Hondt, H.; Abakumov, A. M.; Hadermann, J.; Kalyuzhnaya, A. S.; Rozova, M. G.; Antipov, E. V.; Van Tendeloo, G. *Chem. Mater.* **2008**, *20*, 7188.
(17) Belik, A. A.; Iikubo, S.; Yokosawa, T.; Kodama, K.; Igawa, N.; Shamoto, S.; Azuma, M.; Takano, M.; Kimoto, K.; Matsui, Y.; Takayama-Muromachi, E. *J. Am. Chem. Soc.* **2007**, *129*, 971.
(18) Tanaka, M.; Katsuya, Y.; Yamamoto, A. *Rev. Sci. Instrum.* **2008**, *79*, 075106.
(19) Izumi, F.; Ikeda, T. *Mater. Sci. Forum* **2000**, *321*−*324*, 198.
(20) Dixon, E.; Hadermann, J.; Hayward, M. A. *J. Solid State Chem.* **2011**; doi:10.1016/j.jssc.2011.05.026.
(21) Brese, R. E.; O'Keeffe, M. *Acta Crystallogr., Sect. B* **1991**, *47*, 192.
(22) Okamoto, H.; Imamura, N.; Karppinen, M.; Yamauchi, H.; Fjellvag, H. *J. Solid State Chem.* **2010**, *183*, 186.
(23) Antipov, E. V.; Abakumov, A. M.; Istomin, S. Y. *Inorg. Chem.* **2008**, *47*, 8543.
(24) Aguadero, A.; Falcon, H.; Campos-Martin, J. M.; Al-Zahrani, S. M.; Fierro, J. L. G.; Alonso, J. A. *Angew. Chem., Int. Ed.* **2011**; doi:10.1002/anie.201007941.
(25) Chiba, H.; Atou, T.; Faqir, H.; Kikuchi, M.; Syono, Y.; Murakami, Y.; Shindo, D. *Solid State Ionics* **1998**, *108*, 193.
(26) Montanari, E.; Righi, L.; Calestani, G.; Migliori, A.; Gilioli, E.; Bolzoni, F. *Chem. Mater.* **2005**, *17*, 1765.
(27) Yang, H.; Chi, Z. H.; Li, F. Y.; Jin, C. Q.; Yu, R. C. *Phys. Rev. B* **2006**, *73*, 024114.
(28) Chi, Z. H.; Yang, H.; Li, F. Y.; Yu, R. C.; Jin, C. Q.; Wang, X. H.; Deng, X. Y.; Li, L. T. *J. Phys.: Condens. Matter* **2006**, *18*, 4371.
(29) Yang, H.; Chi, Z. H.; Yao, L. D.; Zhang, W.; Li, F. Y.; Jin, C. Q.; Yu, R. C. *J. Appl. Phys.* **2006**, *100*, 044105.
(30) Yang, H.; Chi, Z. H.; Jiang, J. L.; Feng, W. J.; Dai, J. F.; Jin, C. Q.; Yu, R. C. *J. Mater. Sci.* **2008**, *43*, 3604.
(31) Ge, B. H.; Li, F. H.; Li, X. M.; Wang, Y. M.; Chi, Z. H.; Jin, C. Q. *Chinese Phys. B* **2008**, *17*, 163.
(32) Yokosawa, T.; Belik, A. A.; Asaka, T.; Kimoto, K.; Takayama-Muromachi, E.; Matsui, Y. *Phys. Rev. B* **2008**, *77*, 024111.
(33) Halasyamani, P. S.; Poeppelmeier, K. R. *Chem. Mater.* **1998**, *10*, 2753.
(34) Fischer, P.; Waldner, F. *Solid State Commun.* **1982**, *44*, 657.
(35) Sharan, A.; Lettieri, J.; Jia, Y.; Tian, W.; Pan, X.; Schlom, D. G.; Gopalan, V. *Phys. Rev. B* **2004**, *69*, 214109.
(36) Baettig, P.; Seshadri, R.; Spaldin, N. A. *J. Am. Chem. Soc.* **2007**, *129*, 9854.
(37) Jeen, H. J.; Singh-Bhalla, G.; Mickel, P. R.; Voigt, K.; Morien, C.; Tongay, S.; Hebard, A. F.; Biswas, A. *J. Appl. Phys.* **2011**, *109*, 074104.